

Phosphorescence of a ruthenium(II) hydride-carbonyl complex with 3-hydroxy-2-quinoxalinecarboxylic acid as a co-ligand

Jan G. Małecki,^{*a} Anna Maroń^a and Joachim Kusz^b

^a Department of Crystallography, Institute of Chemistry, University of Silesia, 40-006 Katowice, Poland.

E-mail: gmalecki@us.edu.pl

^b Institute of Physics, University of Silesia, 40-007 Katowice, Poland

DOI: 10.1016/j.mencom.2015.03.007

The [RuH(CO)(hqxc)(PPh₃)₂] complex, where hqxc is 3-hydroxy-2-quinoxalinecarboxylate, exhibits strong phosphorescence (quantum yield $\Phi = 0.0078$) in the solid state giving rise to a significantly Stokes-shifted spectrum (excitation at 484 nm and emission at 687 nm); the lifetime of 6.5 μ s is very long compared with 0.68 ns measured for the free hqxc ligand.

Luminescent ruthenium(II) complexes containing polypyridine ligands such as 2,2-bipyridine or 1,10-phenanthroline have been extensively studied. These complexes exhibit not only fluorescence emission, but phosphorescence emission is frequently detected in room-temperature fluid solution from these complexes and is attributed to low-lying ³MLCT (metal-to-ligand charge-transfer) excited states. The phosphorescence quantum yields range between 10⁻¹ and 10⁻³ and lifetimes are about 1 μ s in room-temperature solution. The selection of N-heterocyclic ligand is the key because it can modulate emissive properties from the MLCT excited state.^{1–8} As distinct from the polypyridine ruthenium(II) complexes, the luminescence ability of the carbonyl phosphine complexes with N-donor ligands are much less studied.^{9–11} It is well known that, for typical luminescent complexes, the highest occupied molecular orbital (HOMO) has a predominant metal *d* character, while the lowest unoccupied orbital (LUMO) is essentially a π^* orbital localized on the N-donor ligand. The photoluminescence (PL) corresponds to the MLCT [*d*_{Ru} → π^* (N-ligand)] transitions. The emissive ruthenium(II) complexes with strong charge-transfer transitions, *i.e.* high extinction coefficients associated with fully allowed charge-transfer transitions, can serve as effective sensitizer units.¹²

The complexes with 3-hydroxy-2-quinoxalinecarboxylic acid ligands can undergo photoinduced proton transfer (PT) reactions, which are recognized as important and fundamental processes in chemistry and biology.¹³ Among them, the simplest and most accessible for investigation is the excited-state intramolecular PT (ESIPT), often occurring in molecules with an intramolecular hydrogen bond involved in enol-to-keto tautomerism. A considerable number of experimental and theoretical studies have been conducted on representative ESIPT molecules, such as salicylamide, 2-(2-hydroxyphenyl)benzoazole and 3-hydroxyflavone derivatives.^{14,15} Since these molecules show intense fluorescence with a large Stokes shift, they have been attracting interest for use in various optical applications and new ESIPT materials are being developed.^{16–19}

The reaction of [RuHCl(CO)(PPh₃)₃] with 3-hydroxy-2-quinoxalinecarboxylic acid (hqxcH) in methanol gave the [RuH(CO)(hqxc)(PPh₃)₂] complex as a red crystalline solid.[†] The complex

was characterized by spectroscopic techniques and single-crystal X-ray analysis.[‡] The IR spectrum of the complex shows bands at 1945 and 1926 cm⁻¹ indicating the hydride and carbonyl ligands, respectively. The ring C=N and C=C stretching modes of the quinoxaline ligand are observed at 1641 cm⁻¹. The stretches of COO⋯HO group gave a band at 1708 cm⁻¹. The position of C=O (from COO) stretching vibration suggests the formation of a

UV-VIS (solid state, λ /nm): 475, 400, 350, 250. UV-VIS [methanol, λ /nm (log ϵ): 466.4 (2.52), 388.8 (3.14), 322.0 (3.70), 276.0 (4.03), 251.2 (4.33), 207.2 (4.85). ¹H NMR (400 MHz, CDCl₃) δ : 14.45 (s, OH), 13.89 (s, OH), 8.68 (d, hqxc, *J* 8.7 Hz), 8.17 (d, hqxc, *J* 8.6 Hz), 7.69 (dd, 17H, *J* 16.4 and 5.7 Hz), 7.64–7.10 (m, PPh₃/hqxc), 6.93 (s, 4H), –10.51 (t, H_{Ru}, *J* 19.1 Hz). ¹³C NMR (101 MHz, CDCl₃) δ : 173.12 (s), 158.68 (s), 143.00 (s), 138.04 (s), 134.29 (s), 133.41 (dt, *J* 8.7 and 6.1 Hz), 132.16 (s), 131.80 (dd, *J* 22.8 and 6.1 Hz), 131.44 (s), 128.09 (q, *J* 4.9 Hz), 127.76 (s), 127.27 (s), 126.87 (s), 126.34 (s). ³¹P NMR (202 MHz, CDCl₃) δ : 43.69 (s). Found (%): C, 65.25; H, 4.52; N, 3.27. Calc. for C₄₆H₃₆N₂O₄P₂Ru (%): C, 65.48; H, 4.30; N, 3.32.

[‡] The X-ray intensity data for [RuH(CO)(hqxc)(PPh₃)₂] were collected on a Gemini A Ultra diffractometer equipped with an Atlas CCD detector using graphite monochromated MoK α radiation ($\lambda = 0.71073$ Å) at room temperature. Lorentz, polarization and empirical absorption correction using spherical harmonics implemented in SCALE3 ABSPACK scaling algorithm (CrysAlis RED, Oxford Diffraction Ltd., Version 1.171.35.21, 2012) were applied. The structure was solved by the direct method and subsequently completed by the difference Fourier recycling. All the non-hydrogen atoms were refined anisotropically using a full-matrix least-squares technique. The hydrogen atoms were treated as riding on their parent carbon atoms and assigned isotropic temperature factors equal to 1.2 times the value of equivalent temperature factor of the parent atom. Knowing about the limits of Fourier synthesis and the problems in recognizing artifacts in the immediate neighborhood of heavy atoms, it is doubtful if a reliable position for the hydrogen atom bound to the Ru-atom can be found in the difference Fourier map avoiding the danger of mistaking the effects of the series termination errors for a true atomic position. In the test complex, the Ru–H bond length of 1.84(3) Å is normal and though that similar distances are present in Cambridge Structural Database (CSD; ConQuest v. 1.15; 2013). SHELXS and SHELXL programs²¹ were used for all the calculations.

Selected crystallographic data for C₄₆H₃₆N₂O₄P₂Ru: monoclinic, space group *C2/c*, *a* = 16.7399(11), *b* = 16.9750(8) and *c* = 27.8949(13) Å, β = 98.329(5)°, *V* = 7843.0(7) Å³, *Z* = 8, *d*_{calc} = 1.429 g cm⁻³, μ = 0.528 mm⁻¹. Data/restraints/parameters: 6937/0/500; *S* = 1.007. Final *R* indices [*I* > 2 σ (*I*)] : *R*₁ = 0.0521, *wR*₂ = 0.1671; *R* indices (all data): *R* = 0.760, *wR* = 0.2070.

CCDC 984595 contains the supplementary crystallographic data for this paper. These data can be obtained free of charge from The Cambridge Crystallographic Data Centre via <http://www.ccdc.cam.ac.uk>.

[†] Methanol solution (70 cm³) of [RuHCl(CO)(PPh₃)₃] (0.2 g, 2 × 10⁻⁴ mol) and 3-hydroxy-2-quinoxalinecarboxylic acid (0.05 g, ~2 × 10⁻⁴ mol) was refluxed for 3 h. The crystals suitable for X-ray analysis were obtained by slow evaporation of the reaction mixture. Yield 82%. IR (KBr, ν /cm⁻¹): 1945 (s, $\nu_{\text{Ru-H}}$), 1926 (s, $\nu_{\text{Ru-CO}}$), 1708 (s, $\nu_{\text{COO/OH}}$), 1641 (s, $\nu_{\text{C=N}}$, $\nu_{\text{C=C}}$).

strong H-bond between hydroxyl and carboxylate groups in the coordinated quinoxaline moiety. 3-Hydroxy-2-quinoxaline-carboxylic acid in the solid state exists in a dimer form; thus, it is difficult to compare the IR bands of free and complex ligands. Nevertheless, in the free acid the band at 1737 cm^{-1} is attributed to C=O stretches²⁰ and the shift of about 30 cm^{-1} confirming that the C=O bond of the complex is weakened. The ^1H and ^{13}C NMR spectra of the complex show signals attributed to quinoxaline and phosphine phenyl rings. The triplet at high field (-10.51 ppm) in the ^1H NMR spectrum confirms the hydride ligand in the coordination sphere of the complex. However, proton signals at 14.45 and 13.89 ppm and a singlet at 173.12 ppm in the ^{13}C NMR spectrum suggest that the 3-hydroxy-2-quinoxalinecarboxylate ligand occurs in solution in two forms. Along with the enol form, the lactam (keto) one exists, in which the proton of the 3-hydroxy group is detached and instead a proton is attached to the quinoxaline ring nitrogen at the 4-position.

The ruthenium(II) ion in the complex has a distorted octahedral geometry, and the complex belongs to the monoclinic $C2/c$ space group (Figure 1).

The bond lengths and angles are comparable with distances in other hydride-carbonyl ruthenium(II) complexes with N-hetero-aromatic ligands. The pseudooctahedral coordination environment on the ruthenium(II) central ion is mainly deviated by a bite angle of 3-hydroxy-2-quinoxalinecarboxylate. The N(1)–Ru(1)–O(2) angle is $74.5(2)^\circ$. The carbonyl group lies in the *trans* position to the nitrogen donor atom of a pyrazine ring, and the oxygen donor atom from the COO group is *trans* to the hydride ligand. The Ru(1)–C(1) and Ru(1)–H(1) distances are 1.867(10) and 1.84(3) Å, respectively. Moreover, the C(1)–O(1) bond length and the Ru(1)–C(1)–O(1) angle are 1.149(9) Å and $177.5(9)^\circ$, respectively. The Ru–C bond distance is normal for a monomeric Ru^{II} carbonyl complex (the distances generally range from 1.74 to 1.98 Å).

In the molecular structure of the complex, three molecular hydrogen bonds are observed, and the hydrogen bond between hydroxyl and carboxyl groups creates the intramolecular ring of $S_1^1(6)a$ type significant from enol-to-keto tautomerism of hqxc ligand.

The complex exhibits emission in both a solid state and solution.⁸ The acetonitrile solution and solid-state samples excited at 487/484 nm gave emission peaks at 747 and 687 nm, respectively.

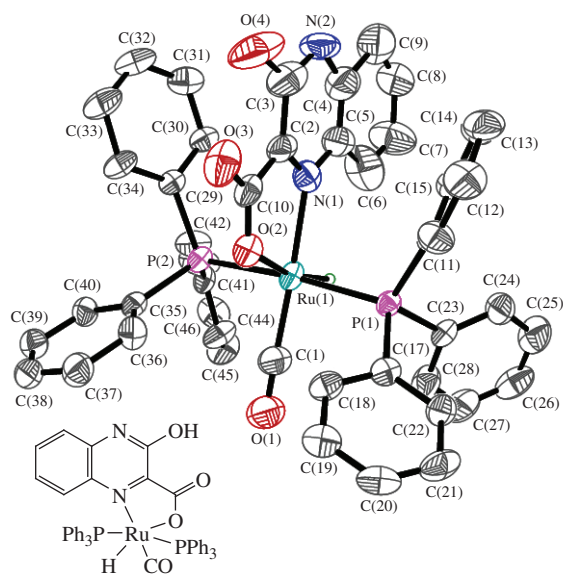


Figure 1 ORTEP plot of the $[\text{RuH}(\text{CO})(\text{hqxc})(\text{PPh}_3)_2]$ complex. The displacement ellipsoids are drawn with a 50% probability. The hydrogen atoms, except of H_{Ru} , are omitted for clarity.

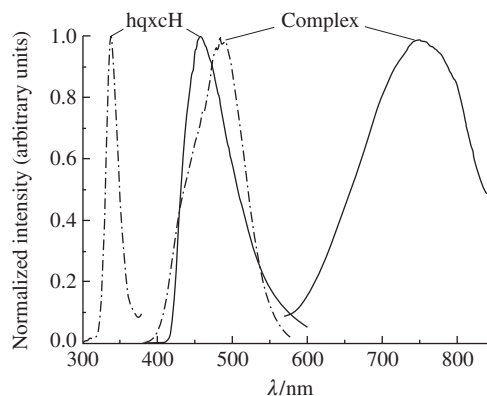


Figure 2 Normalized excitation (dash-dot line) and emission (solid line) spectra of the hqxcH ligand and $[\text{RuH}(\text{CO})(\text{hqxc})(\text{PPh}_3)_2]$ complex in acetonitrile solutions at room temperature.

Table 1 Emission data for the $[\text{RuH}(\text{CO})(\text{hqxc})(\text{PPh}_3)_2]$ complex and the 3-hydroxy-2-quinoxalinecarboxylic acid ligand.

Complex	Temperature/K	$\lambda_{\text{exc}}/\text{nm}$	$\lambda_{\text{em}}/\text{nm}$	$\tau/\mu\text{s}$	$\Phi_{\text{em}}/10^{-2}$
ACN	298	487	747	3.7	0.01
Solid state	298	484	687	6.5	0.78
MeOH–EtOH (1:4)	77	435	670	—	—
ACN ligand	298	338	457	0.68×10^{-3}	1.19
Powder	non-emissive				

Figure 2 shows the excitations and emission spectra of the acetonitrile solutions of 3-hydroxy-2-quinoxalinecarboxylic acid and the $[\text{RuH}(\text{CO})(\text{hqxc})(\text{PPh}_3)_2]$ complex.

The low-temperature spectrum of emission revealed a hypsochromic shift of the excitation and emission maxima (Table 1).

The low-temperature emission spectrum has a typical shape and any vibrational structure is observed. The differences in the emission maxima between solution and solid state can be connected with changes in the strength of the $\text{OH}\cdots\text{COO}$ hydrogen bond depending on polarity of the solvent, particularly, the PL maximum in the solid state is shifted by 60 nm to higher energy compared with solution.

The Stokes shifts calculated from the excitation and emission maxima are 7147 and 6105 cm^{-1} in the solid state and solution, respectively. At 77 K, the shift increases to 8063 cm^{-1} . These values are much larger than those of conventional dyes ($\sim 4000\text{ cm}^{-1}$) and suggest that ESIPT occurs in the complex. 3-Hydroxy-2-quinoxalinecarboxylic acid in the solid state is non-emissive,

⁸ The steady-state emission spectra were measured for solid states and acetonitrile solutions on a FLS-980 spectrofluorimeter at ambient temperature using a Xe lamp as a light source. The low-temperature spectra were measured for EtOH–MeOH (1:4) solutions on a FLS-980 spectrofluorimeter at a temperature of liquid nitrogen. The quantum yields of fluorescence were determined by an absolute method at room temperature using the integrating sphere with solvent (solution) or standard sample (powder) as a blank. The solutions of samples were first filtered and diluted to absorbance under 0.1 to avoid an inner filter effect and the influences of impurities; then they were excited at the excitation wavelength of the complexes. The time-resolved measurement was carried out for optically diluted ($0.05 < \text{O.D.} < 0.1$) acetonitrile solutions or powder solids at room temperature using the time correlated single photon counting methods. The excitation wavelength of the ligand (340 nm) was obtained using a EPLED-340 nm picosecond pulsed diode with a 100 ns pulse period as a light source, and PMT+500 nm (Hamamatsu, R928P) in cooled housing was used as a detector. The excitation wavelength of the complex was obtained using a $\mu\text{F}2$ 60 W xenon flash lamp optimized for multichannel scaling lifetime measurements, and PMT+500 nm in cooled housing was used as a detector.

and in solution exhibits emission with a maximum at 457 nm with excitation at 338 nm. Moreover, the quantum yield measured for the complex solution is significantly lower (0.01%) compared with the ligand (1.19%). The measured lifetimes of 6.5 and 3.7 μ s for the complex in the solid state and solution, respectively, are long especially compared with that of the free ligand (0.68 ns). In the complex, the emission may occur from two excited states 1 CT and 3 CT. In the emission process the ligand triplet state (3 LC) may compromise or even quench luminescence. In this case, the energy difference between 3 LC and 3 MLCT states is important. The energy level difference between the Ru^{II} *d* orbitals and the ligand π orbital may be small enough for thermal activation, assuring electron-configuration transformation between 3 LC and 3 MLCT excited states. In addition, if the energy of the lowest lying excited state of ligand is smaller than that of 3 MLCT, difference between ligand and metal centered triplet states is small that causes the energy transfer between 3 LC and 3 MLCT excited states to become partly irreversible. Considering the radiative and non-radiative decay rates, calculated from experimentally available quantities: $\tau = 1/(k_r + k_{nr})$, $\Phi_{em} = k_r/(k_r + k_{nr})$, equal to 1.2×10^3 and 1.5×10^5 s⁻¹, respectively, we can assume that, in the case of the complex, the 3 MLCT \rightarrow 3 LC non-radiative process plays a substantial role.

References

- 1 S. Perruchas, X. F. L. Goff, S. Maron, I. Maurin, F. Guillen, A. Garcia, T. Gacoin and J.-P. Boilot, *J. Am. Chem. Soc.*, 2010, **132**, 10967.
- 2 N. Armaroli, G. Accorsi, M. Holler, O. Moudam, J.-F. Nierengarten, Z. Zhou, R. T. Wegh and R. Welter, *Adv. Mater.*, 2006, **18**, 1313.
- 3 Q. Zhang, Q. Zhou, Y. Cheng, L. Wang, D. Ma, X. Jing and F. Wang, *Adv. Mater.*, 2004, **16**, 432.
- 4 M. Nishikawa, K. Nomoto, S. Kume, K. Inoue, M. Sakai, M. Fujii and H. Nishihara, *J. Am. Chem. Soc.*, 2010, **132**, 9579.
- 5 J.-L. Chen, B. Wu, W. Gu, X.-F. Cao, H.-R. Wen, R. Hong, J. Liao and B.-T. Su, *Transition Met. Chem.*, 2011, **36**, 379.
- 6 A. A. Karasik, A. S. Balueva, E. I. Musina and O. G. Sinyashin, *Mendeleev Commun.*, 2013, **23**, 237.
- 7 N. N. Solodukhin, V. V. Utochnikova, L. S. Lepnev and N. P. Kuzmina, *Mendeleev Commun.*, 2014, **24**, 91.
- 8 J. G. Małecki, A. Maroń, I. Gryca and M. Serda, *Mendeleev Commun.*, 2014, **24**, 26.
- 9 J. G. Małecki and A. Maroń, *Transition Met. Chem.*, 2012, **37**, 727.
- 10 J. G. Małecki and A. Maroń, *Transition Met. Chem.*, 2013, **38**, 133.
- 11 J. G. Małecki and A. Maroń, *Polyhedron*, 2012, **31**, 44.
- 12 S. Singaravadivel, M. Velayudham, E. Babu, P. Muthu Mareeswaran, K.-L. Lu and S. Rajagopal, *J. Fluoresc.*, 2013, **23**, 1167.
- 13 S. Hammes-Schiffer, *Acc. Chem. Res.*, 2001, **34**, 273.
- 14 S. Nagaoka, A. Nakamura and U. Nagashima, *J. Photochem. Photobiol. A*, 2002, **154**, 23.
- 15 A. S. Klymchenko, V. G. Pivovarenko, T. Ozturk and A. P. Demchenko, *New J. Chem.*, 2003, **27**, 1336.
- 16 S. Park, O.-H. Kwon, S. Kim, S. Park, M.-G. Choi, M. Cha, S. Y. Park and D.-J. Jang, *J. Am. Chem. Soc.*, 2005, **127**, 10070.
- 17 S.-J. Lim, J. Seo and S. Y. Park, *J. Am. Chem. Soc.*, 2006, **128**, 14542.
- 18 K.-Yu Chen, C.-C. Hsieh, Yi-M. Cheng, C.-H. Lai and Pi-T. Chou, *Chem. Commun.*, 2006, 4395.
- 19 A. S. Klymchenko, D. A. Yushchenko and Y. Mely, *J. Photochem. Photobiol. A*, 2007, **192**, 93.
- 20 S. Badoğlu and S. Yurdakul, *Spectrochim. Acta, Part A*, 2013, **101**, 13.
- 21 G. M. Sheldrick, *Acta Crystallogr., Sect. A*, 2008, **64**, 112.

Received: 30th June 2014; Com. 14/4411